UNIVERSITAT POLITÈCNICA DE VALÈNCIA

Thermodynamic analysis and modeling of water vapor adsorption isotherms of roasted specialty coffee (Coffee arabica L. cv. Colombia)

TRABAJO FIN DE MÁSTER UNIVERSITARIO EN CIENCIA E INGENIERÍA DE ALIMENTOS

ALUMNO/A: **GENTIL ANDRES COLLAZOS ESCOBAR**

TUTOR/A ACADEMICO: JOSÉ VICENTE GARCÍA-PÉREZ
COTUTOR/A: JOSÉ BON CORBÍN
COTUTOR EXTERNO/A: NELSON GUTIÉRREZ GUZMÁN
COTUTOR EXTERNO/A: HENRY ALEXANDER VÁQUIRO HERRERA
DIRECTOR EXPERIMENTAL: EDUARDO A. SANCHEZ-TORRES

Curso Académico: 2019-2020

VALENCIA, 11 DE SEPTIEMBRE DE 2020

THERMODYNAMIC ANALYSIS AND MODELING OF WATER VAPOR ADSORPTION ISOTHERMS OF ROASTED SPECIALTY COFFEE (*Coffee arabica* L. cv. Colombia)

Gentil Andres Collazos-Escobar[1*]; Nelson Gutiérrez-Guzmán[1]; Henry Alexander Váquiro-Herrera[2]; Eduardo A. Sanchez-Torres[3] , José Bon Corbín[3]; José V. García-Pérez[3];

RESUMEN

Las isotermas de adsorción de vapor de agua representan una herramienta eficaz y valiosa para predecir el comportamiento higroscópico de los alimentos bajo diferentes humedades y temperaturas. Además, se pueden utilizar para determinar las propiedades termodinámicas efectivas y así, establecer la vida útil y las condiciones de almacenamiento más adecuadas de los alimentos. Los objetivos de este trabajo fueron determinar y modelizar las isotermas de adsorción de vapor de agua y cuantificar las propiedades termodinámicas del café especial tostado. Así, se analizó tanto el café en grano como el molido a tamaños de partícula medio y fino en un rango de actividades de agua entre 0.1–0.9 y temperaturas de 25, 35 y 45 °C. Las isotermas de adsorción se determinaron utilizando el método del punto de rocío dinámico (DDI). La modelización de las isotermas de adsorción se realizó utilizando 10 modelos diferentes para representar la influencia de la actividad del agua y la temperatura en el contenido de humedad de equilibrio. Además, se estudió la capacidad higroscópica del café tostado mediante análisis termodinámico diferencial. Los resultados experimentales y la modelización mostraron que la mayor adsorción de humedad en el café molido se relacionó con una mayor área de adsorción, lo que sugiere que el café especial podría almacenarse de manera más segura en la etapa de grano. El modelo empírico de Peleg fue el más adecuado para representar el comportamiento de adsorción cóncavo ascendente de tipo III y el infecto inverso de la temperatura a altas actividades de agua en las isotermas de adsorción. El análisis termodinámico diferencial indicó un aumento en la energía de adsorción de agua con el descenso del contenido de humedad de equilibrio, mientras que los valores negativos de la energía libre de Gibbs revelaron la espontaneidad del proceso de adsorción.

Palabras clave: procesamiento húmedo, higroscopicidad, área de superficie de adsorción; proceso espontáneo, propiedades diferenciales

ABSTRACT

Water vapor adsorption isotherms represent an effective and valuable tool for predicting the hygroscopic behavior of foods under different humidities and temperatures. Besides, isotherms can be used to determine the effective thermodynamic properties and thus, establish the shelf life and the most suitable storage conditions for food materials. The aims of this work were to determine and model the water vapor adsorption isotherms and to assess the thermodynamic properties of roasted specialty coffee. Thus, both coffee beans and ground coffee at medium and fine particle sizes were analyzed in a range of water activities between

0.1–0.9 and temperatures of 25, 35, and 45 °C. The adsorption isotherms were determined using the dynamic dew point (DDI) method. Modeling of the adsorption isotherms was carried out using 10 different models to represent the influence of the water activity and the temperature on the equilibrium moisture content. Furthermore, the hygroscopic capacity of roasted coffee was analyzed by differential thermodynamic analysis. Experimental results and modeling showed that the higher moisture adsorption found in the ground coffee was related to a larger adsorption area, suggesting that specialty coffee could be stored more safely as beans. The Peleg empirical model was the most suitable to represent the type III upward concave adsorption behavior and the effect of temperature on adsorption isotherms. Differential thermodynamic analysis indicated an increase in water adsorption energy with decreasing equilibrium moisture content, while negative Gibbs free energy values revealed the spontaneity of the adsorption process.

Keywords: wet processing, hygroscopicity, adsorption surface area, spontaneous process, differential properties

RESUM

Les isotermes d'adsorció de vapor d'aigua representen una eina eficaç i valuosa per a predir el comportament higroscòpic dels aliments baix diferents humitats i temperatures. A més, es poden utilitzar per a determinar les propietats termodinàmiques efectives i així, establir la vida útil i les condicions d'emmagatzematge més adequades dels aliments. Els objectius d'aquest treball van ser determinar les isotermes d'adsorció de vapor d'aigua i les propietats termodinàmiques del café especial torrat. Així, es va analitzar tant el café en gra com el molt a grandàries de partícula medie i fi en un rang d'activitats d'aigua entre 0.1–0.9 i temperatures de 25, 35 i 45 °C. Les isotermes d'adsorció es van determinar utilitzant el mètode del punt de rosada dinàmica (DDI). La modelització de les isotermes d'adsorció es va realitzar utilitzant 10 models diferents per a representar la dependència del contingut d'humitat d'equilibri sobre l'activitat de l'aigua i la temperatura. A més, es va estudiar la capacitat higroscòpica del café torrat mitjançant anàlisi termodinàmica diferencial. Els resultats experimentals i la modelització van mostrar que la major adsorció d'humitat en el café molt es va relacionar amb una major àrea d'adsorció, la qual cosa suggereix que el café especial podria emmagatzemar-se de manera més segura en l'etapa de gra. El model empíric de Peleg va ser el més adequat per a representar el comportament d'adsorció còncau ascendent de tipus III i els efectes de la temperatura sobre les isotermes d'adsorció. L'anàlisi termodinàmica diferencial va indicar un augment en l'energia d'adsorció d'aigua amb el descens del contingut d'humitat d'equilibri, mentre que els valors negatius de l'energia lliure de Gibbs van revelar l'espontaneïtat del procés d'adsorció.

Paraules clau: processament humit, higroscopicitat, àrea de superfície d'adsorció; procés espontani, propietats diferencials

[1*]Centro Surcolombiano de Investigación en Café CESURCAFÉ, Universidad Surcolombiana, Neiva-Huila, Colombia. gentil.collazos@usco.edu.co. [2]Facultad de Ingeniería Agronómica, Universidad del Tolima, Ibagué-Tolima, Colombia. [3]Grupo de Análisis y Simulación de Procesos Agroalimentarios (ASPA), Departamento de Tecnología de Alimentos, Universidad Politécnica de Valencia, C/Camino de Vera s/n, 46022 Valencia, Spain.

1. INTRODUCTION

Coffee is economically one of the most important agricultural commodities and Coffea arabica dominates global production. At the same time, the worldwide interest in developing specialty coffee has risen, in a particular case the high-quality Arabica coffee which is characterized for its superior organoleptic qualities (Geeraert et al., 2019). In Colombia, coffee production is an important industry for international trading. The International Coffee Organization considers this country as the main soft coffee exporter; in 2018/2019 the production was 13,858 thousand of 60 kg bags (OIC, 2020). Additionally, the Colombian coffee reputation has become highly differentiated due to its sensorial attributes, such as aroma and body (Özdestan et al., 2013).

The "specialty coffee" mainly refers to a coffee which possess desirable, excellent, unique flavor qualities and specific of a geographical region (Velásquez et al., 2019). The increasing of specialty coffee consumption and demand creates an opportunity for producer countries to obtain higher prices for their harvests in specialized markets (Tolessa et al., 2016).

To preserve the coffee cup quality, it is necessary to control the roasting and further storage, due to this step induces the production and/or degradation of several chemical compounds such as acids, caffeine, lipids, and carbohydrates (Barbosa et al., 2019). Generally, roasted coffee is a highly hygroscopic matrix, readily adsorbing moisture when interacting with its environment during storage (Iaccheri et al., 2015). This property may affect the coffee-freshness modifying its desirable sensory attributes. Whereby, for safe storage, the temperature and relative humidity are indispensable parameters to be considered in the food-surround interactions (Tripetch & Borompichaichartkul, 2019). In this sense, water vapor sorption isotherms depicts the relationship between equilibrium moisture content and water activity at a constant temperature a pressure.

Sorption isotherms are highly suitable to interpret the water sorption mechanism and interactions between water and foodstuff components. Furthermore, it gives relevant insight in drying modeling, optimization, predicting shelf-life, determining critical moisture level, and provides a reliable criterion to the selection of packaging material (Arslan-Tontul, 2020). Several methods are available for the determination of sorption isotherms. The recent technology such as the dynamic dewpoint isotherms (DDI) provides a greater resolution and high-speed analysis (Yao et al., 2020) and a larger number of experimental data (Fan et al., 2017) compared to standard gravimetric method (Mutlu et al 2020).

Modeling of water sorption isotherms is a useful tool for describing and predicting the equilibrium moisture content at different water activity levels and temperatures (Aouaini et al., 2015). Different mathematical sorption models are widely used. However, due to the food complexity, there is not a unique model to represent the sorption isotherms of all agricultural products (Bon et al., 2012). Literature report several uses of the theoretical Guggenheim-

Anderson-de Boer (GAB) model (Červenka et al., 2015), which can be applied in a wide water activity range. Besides the GAB model is frequently preferred for it provides a monolayer moisture content parameter highly related to the stability of the food material (Červenka et al., 2019). Otherwise, numerous empirical (Smith and Oswin) and semiempirical (Halsey and Henderson) models are available to predict the moisture properties of foods (Yogendrarajah et al., 2015).

From water sorption isotherms at different temperatures; thermodynamic properties can also be predicted, which constitutes a relevant information for storage stability and shelf-life of dehydrated food products (Velázquez-Gutiérrez et al., 2015). Consequently, the thermodynamic analysis of sorption data provides an approximate perspective into the microstructure and evidences the water-substrate interaction on the food matrix interface. In this sense, the net isosteric heat of sorption or differential enthalpy and differential entropy describe the water-binding energy with the food structure, which represents a key information for assessing the energy requirements of heat and mass transfer during dehydration (Červenka et al., 2019).

Changes of the differential enthalpy provide a measurement of the energy variations occurring on the interactions of water molecules with the sorbent during the sorption process while, the differential entropy may be associated with interfacial spatial arrangements of water, relating the binding or repulsive forces in the system (Rodríguez-Bernal et al., 2015). Finally, the affinity of the sorbents by water and the spontaneity of the sorption process can be explained through Gibbs free energy, which is defined as the total energy required to transfer water molecules from the vapor state to the solid surface or vice-versa (Bastıoğlu et al., 2017).

As already mentioned, it is highly relevant to understand the hygroscopic properties of roasted coffee in order to establish optimal storage conditions and guaranteeing sensory-quality. In this sense, the aims of this work were: (i) to determine the water vapor adsorption isotherms of roasted coffee beans and ground roasted coffee at temperatures of 25, 35 and 45 °C and water activities between 0.1–0.9 using the DDI method; (ii) to analyze the feasibility of different mathematical sorption models to represent the influence of the water activity and temperature on the equilibrium moisture content and (iii) to assess the hygroscopic capacity of roasted coffee through differential thermodynamic analysis.

2. MATERIALS AND METHODS

2.1 Coffee processing

Nine coffee samples (10 kg) of Colombia variety (*Coffee arabica* L.), from different growing areas in Huila region of Colombia, were processed by the wet method (Velásquez et al., 2019). Each coffee beans samples were pulped with a pulping machine (Gaviota 300, Ingesec, Colombia) and fermented in

plastics containers for 18 h (Velásquez et al., 2019). Subsequently, fermented beans were washed and sun-dried until reaching a moisture content of 10–12 (% w.b.) Moisture evolution during drying was monitored with the handled portable grain moisture tester (Kett PM−450, Science of Sensing, Japan). The sun-drying process was conducted between 9 am to 4 pm daily and the room conditions were 37 ± 3 °C and 25–45% relative humidity. Samples were sensory analyzed according to the Specialty Coffee Association methodology (SCA, 2020), in the Centro Surcolombiano de Investigación en Café (CESURCAFÉ) by five highly trained coffee-sensory panelists (Di Donfrancesco et al., 2014) and classified as specialty coffee. The origin and cup quality score of coffee samples are shown in Table 1.

TABLE 1. Coffee samples characteristics and sensory classification

Sample	Origin	Cup score	Classification
1	Cerro Neiva	86	Specialty coffee
2	Cerro Neiva	88	Specialty coffee
3	Tello	85.75	Specialty coffee
4	Colombia	84.5	Specialty coffee
5	Santa María	84	Specialty coffee
6	Palermo	84	Specialty coffee
7	Palermo	84.75	Specialty coffee
8	San Agustín	84.5	Specialty coffee
9	San Agustín	86.5	Specialty coffee

2.1.1 ROASTING AND GRINDING CONDITIONS

Previously to roasting, the beans were hulled in a laboratory hulling machine (ING-C-250, Ingesec, Colombia). For each sample, 150 g of healthy green coffee beans were roasted using a laboratory equipment (TC-150R, Quantik, Colombia), equipped with a digital display to controlled time and temperature. The roasting program consisted on the preheating of the rotary system at 150 °C for 10 min, heating until 185 ± 2 °C and cooling to 178 ± 2 °C and then, the samples were loaded into the roasting chamber. During roasting, the temperature points were automatically registered every 5 s. After 3.5 min of roasting, the heating was increased from 10 to 60% and was ended when the total process time and temperature were 9 ± 0.5 min and 183 ± 2 °C, respectively.

The coffee samples were roasted at a medium roasting degree, which considers a luminosity (L*) coordinate value between 18 and 25 (Craig et al (2018). To verify this roasting level, the spectrocolorimeter (CR–410, Konica Minolta, N.J. USA) was used considering standard light source D65 and standard observer 10°. Previously, the instrument calibration was performed with a standard white plate (Y = 87.0, x = 0.3160, y = 0.3231). The roasted coffee beans were independently ground in a milling device (Bunn G3 HD-Coffee Mill, Springfield, IL. USA) and separated to medium size particle (particles retained in a #20 standard sieve with a hole diameter of 850 μm) and

fine (particles retained in a #30 standard sieve with a hole diameter of 600 μm). To achieve, the samples were shaken using shaking cycles on a vibratory sieve shaker (EFL-2000, Endecotts LTD, London, U.K) for 10 min.

2.2 Initial moisture content and water activity

The moisture content was determined by drying 5.0 g of samples in an oven (UF55, Memmert GmbH + Co.KG, Schwabach, Germany) at 105 ± 1 °C until constant weight (Mutlu et al., 2020). All gravimetric determinations were made in triplicate and the results were expressed as percentage of dry basis (% d.b.). For water activity (a_w) measurements, a vapor sorption analyzer (VSA Aqualab, Decagon Devices, Inc. Pullman, WA) was used.

2.3 Experimental determination of the water vapor adsorption isotherms

The water vapor adsorption isotherms were determined with the dynamic dewpoint isotherm (DDI) method, using a vapor sorption analyzer (VSA Aqualab Decagon Devices, Inc. Pullman, WA). All tests were performed in triplicate and a water activity range between 0.1–0.9 with intervals of 0.01 a_w, and temperatures of 25, 35, and 45 °C, under an air flow of 100 mL min^{-1}. In every test, samples of 3.5 g of roasted coffee beans and ground roasted-coffee (medium and fine particle size) were placed inside of VSA instrument.

2.4 Mathematical modeling

The water vapor adsorption isotherms of roasted and ground coffee samples were mathematically represented using the ten models shown in Table 2. Where X_e is the equilibrium moisture content (% d.b.), a_w is the water activity, X_m is the monolayer equilibrium moisture content (% d.b.), K, K_0, C and C_0 are the Guggenheim-Anderson-de Boer (GAB) model parameters, H_m and H_n are the water sorption heats of the monolayer and multilayer (kJ mol^{-1}), respectively, L_r is the latent heat of vaporization of pure water (kJ mol^{-1}), T is the absolute temperature (K). While, the b_i terms represent the parameters for the empirical models in which the temperature dependence was assumed to be linear according to Collazos-Escobar et al (2019).

TABLE 2. Mathematical models used to represent the water vapor sorption isotherms of coffee in different processing stages

Model	Mathematical expression	Reference	Eq. No
GAB	$X_e = \dfrac{X_m\, CKa_w}{(1 - Ka_w)(1 + (C - 1)Ka_w)}$ $C = C_0 \exp(\dfrac{H_m - H_n}{RT})$ $K = K_0 \exp(\dfrac{L_r - H_n}{RT})$	(Clemente et al., 2009)	1
Iglesias and Chirife	$X_e = b_1 + b_2\left(\dfrac{a_w}{1 - a_w}\right)$	(Arslan-Tontul, 2020)	2
Halsey	$X_e = \left(\dfrac{-b_1}{\ln a_w}\right)^{1/b_2}$	(Fan et al., 2019)	3
Smith	$X_e = b_1 - b_2 \ln(1 - a_w)$	(Arslan-Tontul, 2020)	4
Oswin	$X_e = b_1\left(\dfrac{a_w}{1 - a_w}\right)^{b_2}$	(Domian et al., 2018)	5
Henderson	$X_e = \left[\dfrac{-\ln(1 - a_w)}{b_1}\right]^{1/b_2}$	(Fan et al., 2019)	6
Peleg	$X_e = b_0 a_w{}^{b_1} + b_2 a_w{}^{b_3}$	(Arslan-Tontul, 2020)	7
Kuhn	$X_e = \left(\dfrac{b_1}{\ln a_w} + b_2\right)$	(Domian et al., 2018)	8
White and Eyring	$X_e = \dfrac{1}{(b_1 + b_2 a_w)}$	(Arslan-Tontul, 2020)	9
DLP	$X_e = b_0 + b_1 x + b_2 x^2 + b_3 x^3$ $x = \ln(-\ln a_w)$	(Yogendrarajah et al., 2015)	10

2.4.1 PARAMETER ESTIMATION AND STATISTICAL ANALYSIS

The nonlinear regression analysis was performed with MATLAB® R2019b (The MathWorks Inc., Natick, MA, USA). The Curve Fitting tool was used to identify the model parameters and calculate the 95% confidence intervals for the non-linear regression analysis. The coefficient of determination (R^2_{adj}) (Eq.11), and root mean square error (RMSE) (Eq.12), were considered to evaluate the goodness of the model fitting. According to Sormoli & Langrish (2015) the minimum RMSE (< 10% d.b.) and maximum R^2_{adj} ($R^2_{adj} > 0.98$) can be considered as a reasonably satisfactory fit.

$$R^2_{adj} = 1 - \left(\frac{N-1}{N-M}\right)(1 - R^2) \tag{11}$$

$$\text{RMSE} = \sqrt{\frac{1}{N}\Sigma_{i=1}^{N}(X_{exp} - X_{pred})^2} \qquad (12)$$

where X_{exp} and X_{pred} are the experimental and predicted equilibrium moisture content (% d.b.), respectively. N is the number of experimental data points; M is the number of model parameters estimated and R^2 is the coefficient of determination between experimental and predicted values.

2.5 Adsorption surface area

Adsorption surface area S_A (m^2 g^{-1} dry basis) of roasted coffee beans and ground roasted coffee was calculated with (Eq.13), according to Tao et al (2018), using the monolayer moisture content from linearized BET model (Eq. 14) evaluated at 25 °C.

$$S_A = X_{mBET}\left(\frac{1}{M_w}\right)N_0 A_W \qquad (13)$$

$$\frac{a_w}{(1-a_w)X_e} = \frac{1}{X_{mBET}C_{BET}} + \frac{C_{BET}-1}{X_{mBET}C_{BET}}a_w \qquad (14)$$

where, X_{mBET} is the monolayer equilibrium moisture content (% d.b.), M_w is the molecular weight of water (kg mol^{-1}), N_0 is the Avogadro number (6×10^{23} molecules mol^{-1}), A_W is the area for a water molecule (1.06×10^{-19} m^2 molecule^{-1}), and C_{BET} is the BET model parameter.

2.6 Thermodynamic analysis

The hygroscopic capacity of roasted specialty coffee was computed by differential thermodynamic analysis; as the water vapor adsorption isotherms were obtained at different temperatures, these properties can be estimated. The net isosteric heat of adsorption, or enthalpy of adsorption (q_{st}), was calculated using the Clausius-Clapeyron equation (Eq. 15), obtained from the slope and intercept of the fitting line of ln (a_w) as function of 1/T at a constant equilibrium moisture content (Červenka et al., 2019).

Gibbs free energy (ΔG) is linked to the spontaneity nature of the water vapor sorption process, which was calculated by the Gibbs equation (Eq. 16). While, the change of differential adsorption entropy (ΔS$_d$) can be calculated from Eq. 17.

$$q_{st} = -R\left[\frac{\partial(\ln a_w)}{\partial\left(\frac{1}{T}\right)}\right]_{X_e} \qquad (15)$$

$$\Delta G = RT \ln(a_w) \qquad (16)$$

$$\Delta S_d = \frac{q_{st}-\Delta G}{T} \qquad (17)$$

where, a_w is water activity, R is the universal gas constant of water vapor (8.314×10^{-3} kJ mol^{-1} K^{-1}), T is the absolute temperature (K) and X_e is the equilibrium moisture content (% d.b.).

3. Results and discussion

3.1 Experimental water vapor adsorption isotherms and modeling

The water vapor adsorption isotherms of roasted and ground specialty coffee samples are shown in Figure 1. It can be observed the J-Curve shape of the isotherms, following a type III form according to Brunauer-Emmett-Teller (BET) classification, which is characteristic of mainly crystalline matrixes and representative of food products rich in soluble components such as sugars (Herman et al., 2018). Similar adsorption isotherms were also obtained by Iaccheri et al (2019) in green and roasted coffee beans, Yogendrarajah et al (2015) in whole black peppercorns, and Collazos-Escobar et al (2020) in dried and roasted cocoa beans. This sorption shape can be explained due to the chemical transformation that the coffee undergoes during the roasting process attributed to Maillard reaction and caramelization of sugars (García-Alamilla et al., 2017). According to Domian et al (2018), it is widely accepted the reduction in the amount of adsorbed water when temperature increases at constant water activity. In this sense, foodstuffs adsorb more water at a low temperature, which indicates that the water molecules at high temperature have higher kinetic energy, enough to overcome the one linked to the sorption site. Thereby, the food product becomes less hygroscopic as a result of the temperature increase. As illustrated in Figure 1b and 1c, at low water activity, the influence of the temperature on the isotherms follows the typical behaviour aforementioned. For coffee beans (Figure 1a), isotherms at different temperatures completely overlap. In any case, the effect of the temperature on the adsorption isotherm at low water activities (0.1–0.6 a_w for coffee beans and 0.1–0.52 a_w for ground coffee) was not significant (p>0.05).

As water adsorption progresses, at high water activities (a_w>0.6 for roasted coffee beans and a_w>0.52 for ground coffee), the typical effect of the temperature was not found. In this case, an inverse phenomenon is illustrated, and the rise of temperature at constant water activity, results in higher equilibrium moisture content, and as consequence, larger water availability.

This fact leads to the crossing of the isotherms-curves at the different temperatures, as is observed in Figure 1b and 1c. These results can be explained in terms of the solubilization of sugars contained in the food matrix at high temperature and water activity. Indeed, at high water activity, the water molecules can be available as a solvent of solutes with a low molecular weight (Domian et al., 2018). The inverse effect of the temperature has been reported in several food and agricultural products: whole black peppercorns (Yogendrarajah et al., 2015), green and roasted yerba mate (Červenka et al., 2015), starch albumen powder (Shittu et al., 2015), spray-dried fat-filled pea

protein-based powders (Domian et al., 2018), borojó fruit and gum arabic powders (Rodríguez-Bernal et al., 2015), and roasted cocoa beans (Collazos-Escobar et al., 2020). Therefore, the sugars dissolution at high water activity and the interactions of adsorbate-adsorbent affect the adsorption mechanism.
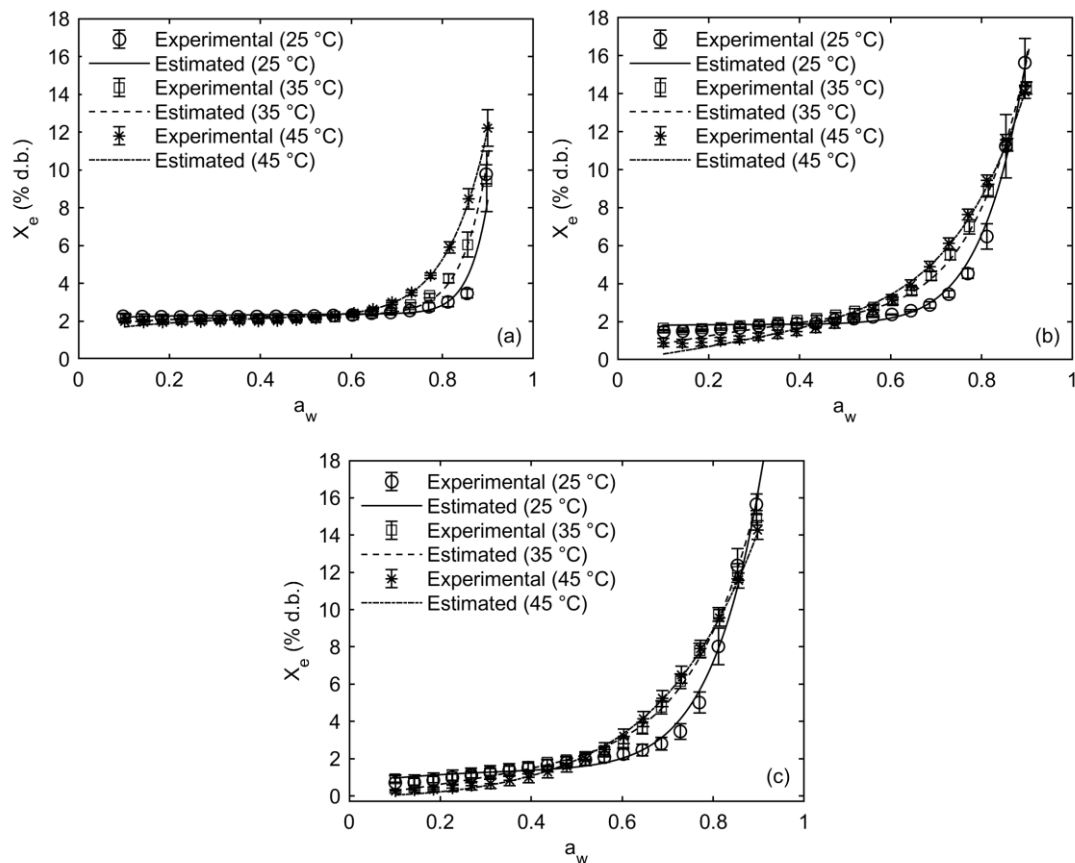

Figure 1. Experimental water vapor adsorption isotherms and Peleg model fitting of roasted coffee beans (a), medium ground roasted coffee (b) and fine ground roasted coffee (c) at 25, 35 and 45 °C

As for the structural effect and its influence in the hygroscopicity capacity of beans and ground coffee, Figure 1a showed an asymptotical evolution of equilibrium moisture content of roasted coffee beans in water activities between 0.1–0.6. Thereby, the equilibrium moisture content remained almost constant varying water activity, showing that the bean structure manifested a low water adsorption capacity respect to the same ground product and experimental conditions. Likewise, slight differences in concave upward J-shape type III isotherms between roasted coffee beans and ground-roasted were also found, as illustrated in Figure 1. These results were interesting due to its contribution to explaining the hygroscopic behavior of roasted coffee, which will be discussed later.

Tables 3, 4 and 5 show the modeling results of water isotherms considering the temperature effect on water vapor adsorption isotherms of roasted and

ground specialty coffee. As already explained, the criteria to select the best model were the lowest error (RMSE) and the highest R^2_{adj}. In this sense, the modeling results reported that the Peleg model provided a satisfactory description of the adsorption behavior of roasted coffee beans (R^2_{adj} = 0.96 and RMSE = 0.49% d.b.) and ground-roasted coffee at medium (R^2_{adj} = 0.98 and RMSE = 0.53% d.b.) and fine particle size (R^2_{adj} = 0.99 and RMSE = 0.44% d.b.).

The goodness of Peleg model fitting is illustrated in Figure 1 in which modelling and experimental results are plotted together. The fitting-capacity of the Peleg equation has been successfully evidenced in roasted coffee beans and ground (Mutlu et al., 2020), and another agricultural product, such as whole black peppercorns (Yogendrarajah et al., 2015) and microencapsulated extra virgin olive oil (Bastıoğlu et al., 2017). On the one hand, in the case of the rest of empirical equations, the DLP model for roasted coffee beans and Iglesias & Chirife, Oswin, Kuhn, White & Eiring and DLP for ground-roasted coffee at medium and fine particle size, could also be considered for representing the adsorption isotherms for practical purposes, due to their adequate fitting capacity. On the other hand, the statistics of the other three empirical models (Smith, Henderson, and Halsey), did no evidence good correspondence between experimental and estimated adsorption data and should not be chosen for representing hygroscopic behavior of specialty coffee.

The theoretical GAB model is widely used to represent the hygroscopicity of most food products (Yogendrarajah et al., 2015). The results obtained in Tables 3, 4, and 5 showed that the generalized GAB model did not fit well the water vapor adsorption isotherms for roasted specialty coffee. Thus, GAB model provided a low R^2_{adj} < 0.95 and RMSE near to 1% d.b, which can be considered as poor fitting parameters compared to Peleg equation. However, the GAB model also provides X_m parameter, which can be considered as useful for determining an adequate moisture content for ensuring stability and good storage in dehydrated food products (Yogendrarajah et al., 2015). Thus, X_m were of 0.85% d.b. for roasted coffee beans, 1.27% d.b. and 1.28% d.b. for ground roasted coffee at medium and fine particle size, respectively; indicating that the lower the particle size, the higher the X_m values. This fact agrees with the results obtained by Mutlu et al (2020), in roasted coffee beans and ground coffee, who attributed this trend to the increasing moisture adsorption surface area in ground coffee compared to roasted coffee beans samples, caused by the grinding process.

TABLE 3. Estimated model parameters and statistical results of roasted coffee beans

Model	Parameters	Confidence Intervals 95%	R^2_{adj}	RMSE (% d.b.)
GAB	$X_m = 0.85\%$ d.b. $C_0 = 101$ $K_0 = 433$ $H_m = 198.6$ kJ mol^{-1} $H_n = 59.1$ kJ mol^{-1}	$[0.82, 0.88]$ $[-1.886 \times 10^8, 1.886 \times 10^8]$ $[390, 477]$ $[-356.8 \times 10^6, 356.8 \times 10^6]$ $[58.8, 59.4]$	0.89	0.77
Iglesias & Chirife	$b_{2.1} = -7.6$ $b_2 = 0.028$ K^{-1} $b_{1.1} = 7$ $b_1 = -0.02$ K^{-1}	$[-8.6, -6.6]$ $[0.024, 0.03]$ $[3, 11]$ $[-0.03, -6.23 \times 10^{-3}]$	0.89	0.76
Oswin	$b_{2.1} = -2$ $b_2 = 9.15 \times 10^{-3}$ K^{-1} $b_1 = 5.09 \times 10^{-3}$ K^{-1}	$[-2.31, -1.67]$ $[8.11 \times 10^{-3}, 0.01]$ $[4.66 \times 10^{-3}, 5.53 \times 10^{-3}]$	0.85	0.88
Peleg	$b_{3.1} = -1.4$ $b_3 = 4.85 \times 10^{-3}$ K^{-1} $b_{2.1} = 2.45$ $b_{1.1} = 198$ $b_1 = -0.6$ K^{-1} $b_{0.1} = 545$ $b_0 = -1.62$ K^{-1}	$[-2.7, -0.1]$ $[7.83 \times 10^{-4}, 8.92 \times 10^{-3}]$ $[2.34, 2.57]$ $[174, 222]$ $[-0.7, -0.5]$ $[381, 710]$ $[-2.14, -1.11]$	0.96	0.49
Kuhn	$b_{2.1} = 10.2$ $b_2 = -0.032$ K^{-1} $b_{1.1} = 7.5$ $b_1 = -0.027$ K^{-1}	$[5.6, 14.8]$ $[-0.046, -0.017]$ $[6.5, 8.5]$ $[-0.03, -0.024]$	0.89	0.77
White & Eiring	$b_{2.1} = -9.6$ $b_2 = 0.027$ K^{-1} $b_{1.1} = 9.5$ $b_1 = -0.03$ K^{-1}	$[-11.8, -7.4]$ $[0.02, 0.03]$ $[7.6, 11.4]$ $[-0.03, -0.02]$	0.90	0.72
DLP	$b_{3.1} = -9.2$ $b_3 = 0.027$ K^{-1} $b_{2.1} = -31.6$ $b_2 = 0.101$ K^{-1} $b_{1.1} = 6.68$ $b_1 = -0.02$ K^{-1} $b_{0.1} = 17.1$ $b_0 = -0.05$ K^{-1}	$[-12.5, -5.9]$ $[0.016, 0.037]$ $[-39.7, -23.5]$ $[0.075, 0.013]$ $[1.24, 12.11]$ $[-0.04, -3.06 \times 10^{-3}]$ $[12.8, 21.3]$ $[-0.06, -0.03]$	0.95	0.54

TABLE 4. Estimated model parameters and statistical results of ground roasted coffee at medium particle size

Model	Parameters	Confidence Intervals 95%	R^2_{adj}	RMSE (% d.b.)
GAB	X_m = 1.27% d.b. C_0 = 114.8 K_0 = 188.2 H_m = 301.4 kJ mol^{-1} H_n = 56.9 kJ mol^{-1}	[1.23, 1.3] $[-1.7 \times 10^8, 1.7 \times 10^8]$ [174.8, 201.6] $[-416.8 \times 10^6, 416.6 \times 10^6]$ [56.7, 57.1]	0.94	0.92
Iglesias & Chirife	$b_2 = 5.62 \times 10^{-3}$ K^{-1} $b_{1.1}$ = −6.1 b_1 = 0.02 K^{-1}	$[5.52 \times 10^{-4}, 5.72 \times 10^{-3}]$ [−8.4, −3.7] [0.01, 0.03]	0.95	0.80
Oswin	$b_{2.1}$ = 3.3 $b_2 = -7.68 \times 10^{-3}$ K^{-1} $b_{1.1}$ = −15.8 b_1 = 0.06 K^{-1}	[2.8, 3.8] $[-9.35 \times 10^{-3}, -6.02 \times 10^{-3}]$ [−19.1, −12.5] [0.05, 0.07]	0.95	0.80
Peleg	$b_{3.1}$ = −17.8 b_3 = 0.06 K^{-1} $b_{2.1}$ = −42 b_2 = 0.15 K^{-1} $b_{1.1}$ = 56.7 b_1 = −0.16 K^{-1} $b_{0.1}$ = 317 b_0 = −0.94 K^{-1}	[−20.9, −14.8] [0.05, 0.07] [−53, −32] [0.11, 0.18] [47.3, 66] [−0.19, −0.13] [282, 352] [−1.1, −0.82]	0.98	0.53
Kuhn	$b_{2.1}$ = −5.95 b_2 = 0.019 K^{-1} $b_1 = -5.55 \times 10^{-3}$ K^{-1}	[−8.33, −3.58] [0.011, 0.027] $[-5.64 \times 10^{-3}, -5.45 \times 10^{-3}]$	0.95	0.82
White & Eiring	$b_{2.1}$ = −5.48 b_2 = 0.015 K^{-1} $b_{1.1}$ = 4.9 b_1 = −0.013 K^{-1}	[−6.29, −4.67] [0.013, 0.018] [4.2, 5.6] [−0.016, −0.011]	0.95	0.82
DLP	$b_{3.1}$ = −27 b_3 = 0.086 K^{-1} $b_{2.1}$ = −39 b_2 = 0.13 K^{-1} $b_{1.1}$ = 30 b_1 = −0.1 K^{-1} $b_{0.1}$ = 14 b_0 = −0.04 K^{-1}	[−30, −24] [0.076, 0.096] [−46, −32] [0.11, 0.15] [26, 34] [−0.12, −0.1] [11, 17] [−0.05, −0.03]	0.98	0.55

TABLE 5. Estimated model parameters and statistical results of ground roasted coffee at fine particle size

Model	Parameters	Confidence Intervals 95%	R^2_{adj}	RMSE (% d.b.)
GAB	$X_m = 1.28\%$ d.b. $C_0 = 99$ $K_0 = 196$ $H_m = 400$ kJ mol^{-1} $H_n = 57$ kJ mol^{-1}	[1.24, 1.32] $[-1.75 \times 10^8, 1.75 \times 10^8]$ [179, 213] $[-727 \times 10^6, 727 \times 10^6]$ [56.8, 57.2]	0.92	1.1
Iglesias & Chirife	$b_2 = 6.08 \times 10^{-3}$ K^{-1} $b_{1.1} = -3.76$ $b_1 = 0.01$ K^{-1}	$[5.98 \times 10^{-3}, 6.17 \times 10^{-3}]$ $[-5.97, -1.54]$ $[5.72 \times 10^{-3}, 0.02]$	0.96	0.80
Oswin	$b_{2.1} = 4.03$ $b_2 = -0.01$ K^{-1} $b_{1.1} = -18.62$ $b_1 = 0.07$ K^{-1}	[3.62, 4.45] $[-0.01, -8.69 \times 10^{-3}]$ $[-21.18, -16.06]$ [0.06, 0.08]	0.97	0.73
Peleg	$b_{3.1} = -27.84$ $b_3 = 0.09$ K^{-1} $b_{2.1} = -75.3$ $b_2 = 0.26$ K^{-1} $b_{1.1} = 52$ $b_1 = -0.15$ K^{-1} $b_{0.1} = 335$ $b_0 = -1$ K^{-1}	$[-30.42, -25.27]$ [0.09, 0.1] $[-86.2, -64.4]$ [0.22, 0.3] [46, 58] $[-0.17, -0.13]$ [310, 360] $[-1.08, -0.92]$	0.99	0.44
Kuhn	$b_{2.1} = -3.6$ $b_2 = 0.01$ K^{-1} $b_1 = -6 \times 10^{-3}$ K^{-1}	$[-5.9, -1.4]$ $[2.8 \times 10^{-3}, 0.02]$ $[-6.08 \times 10^{-3}, -5.9 \times 10^{-3}]$	0.96	0.80
White & Eiring	$b_{2.1} = -3.2$ $b_2 = 7.84 \times 10^{-3}$ K^{-1} $b_{1.1} = 3$ $b_1 = -7.13 \times 10^{-3}$ K^{-1}	$[-4.1, -2.3]$ $[4.88 \times 10^{-3}, 0.01]$ [2.1, 3.9] $[-9.74 \times 10^{-3}, -4.53 \times 10^{-3}]$	0.92	1.07
DLP	$b_{3.1} = -22$ $b_3 = 0.07$ K^{-1} $b_{2.1} = -28.6$ $b_2 = 0.10$ K^{-1} $b_{1.1} = 26.7$ $b_1 = -0.09$ K^{-1} $b_{0.1} = 9.36$ $b_0 = -0.027$ K^{-1}	$[-25, -19]$ [0.06, 0.08] $[-35.3, -21.9]$ [0.08, 0.12] [22.6, 30.8] $[-0.11, -0.08]$ [6.79, 11.92] $[-0.035, -0.019]$	0.98	0.58

3.2 Adsorption surface area

Specific surface area of adsorption S_A for roasted coffee was calculated using the monolayer equilibrium moisture content from the linearized BET model (Eq. 14), in water activities between 0.1–0.6 for roasted coffee beans and 0.1–0.52 a_w for ground coffee, where the usual sorption behavior was found. Similarly to X_m values obtained by the generalized GAB model (Table 3, 4 and 5); the X_{mBET} values at 25 °C were 0.81, 1.04, and 1.16 (% d.b.) for roasted coffee beans and ground roasted coffee at medium and fine particle size, respectively, which corresponds to adsorption surface areas of 28.5,

36.8, and 40.9 (m^2 g^{-1} dry matter.). Thereby, the adsorption surface area increased with the reduction of the particle size. The results were similar to the ones reported in roasted coffee beans and ground coffee at 25 °C by Mutlu et al (2020), who mentioned that the ground coffee samples could bound more water molecules than roasted coffee beans, due to the ground material contains more active adsorption sites, such as the hydroxyl group. Additionally, Tao et al (2018) mentioned in blueberry powders, that the increase in water holding capacity of food powders could be ascribed to the decrease in particle size and the increase of surface area.

3.3 Differential thermodynamic analysis

The variations of the net isoteric heat of adsorption and differential adsorption entropy of roasted coffee beans and ground roasted at different particle sizes are shown in Figure 2.
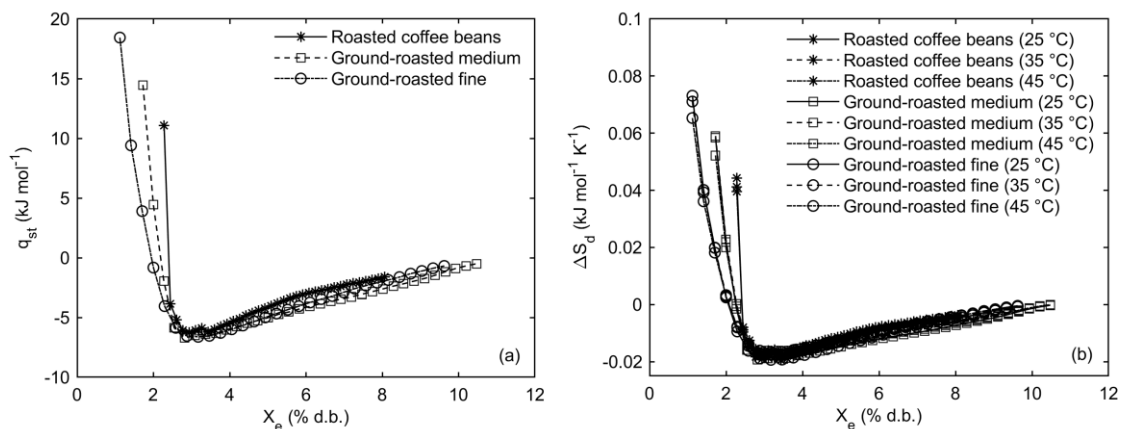
FIGURE 2. Net isosteric heat of adsorption (a), and differential adsorption entropy (b) at 25, 35 and 45 °C of roasted specialty coffee as a function of the equilibrium moisture content.

The net isosteric heat of adsorption (q_{st}) was estimated according to Eq. (15) and plotted as a function of the equilibrium moisture content (Figure 2a). It can be observed the decrease in q_{st} with the increase of the equilibrium moisture content for roasted coffee at low moisture content , between 1.1% d.b to 2% d.b (Figure 2a), evidencing a normal sorption trend. This result can be explained by considering that at low equilibrium moisture contents, the active sorption sites at the surface can strongly bond the water molecules forming mono-molecular layer.

As adsorption progresses, once these highly-energy sites have been occupied, the lower energy sites are exposed as a result of increments in the moisture content (Červenka et al., 2019). Similar results have been reported in the literature for different foodstuffs and agricultural products: green and roasted yerba mate (Červenka et al., 2015), roasted and unroasted carob (Červenka et al., 2019), dried and roasted cocoa beans (Collazos-Escobar et

al., 2020), whole chia seeds (Arslan-Tontul., 2020), whole black peppercorns (Yogendrarajah et al., 2015), and blueberry powders (Tao et al., 2018). Additionally, as can be observed from moisture contents higher than 2%, the water adsorption resulted in the increase of q_{st}, indicating an inverse effect in the normal thermodynamic behavior. The negative values of q_{st} can be explained by the inverse temperature effect on the vapor adsorption isotherms at high water activities, as previously shown in Figure 1. The tendency observed were similar to the ones reported in roasted cocoa beans (Collazos-Escobar et al., 2020) and spray-dried fat-filled pea protein-based powder (Domian et al., 2018). Previous literature also ascribed the inverse effect of the temperature to the solute dissolution at high water activities.

Figure 2b shows the differential adsorption entropy (ΔS_d) variations at different temperatures. ΔS_d decreased as the moisture content was increased and the temperature influence was not significant ($p > 0.05$). As can be observed in Figure 2b, in the moisture content range of 1.1% d.b to 2% d.b, the differences of ΔS_d of coffee beans and ground roasted coffee was evident. According to Yogendrarajah et al (2015), sorption entropy can be considered as proportional to the number of available sorption sites at a specific energy level. Thereby, the results suggested that the fine particle size at a certain energy level had more number of available sorption sites respect to medium particle size and roasted beans. This result can be explained due to the adsorption surface area results mentioned above (see section 3.2). Additionally, ΔS_d negative values were observed in equilibrium moisture content above 2% d.b. This fact can be explained due to changes in water vapor adsorption trend corresponding to the inverse effect of temperature observed in Figures 1a, 1b, and 1c.

This result is consistent with the data reported by Červenka et al (2015), who mentioned that the changes caused by roasting may promote the dissolution of sugars at high water activities and temperatures causing changes in the sorption properties. The results observed in Figure 2b were similar to the reported by Collazos-Escobar et al (2020) in roasted and raw cocoa beans, who found the inverse adsorption phenomenon for water activities higher than 0.8. Collazos-Escobar et al (2020) claimed that the modification of differential thermodynamic properties when the cocoa beans linked to the roasting process could be ascribed to the dissolution of sugars and other water soluble components. If roasted coffee and cocoa are compared, the a_w point wherein the inverse adsorption behavior occurred was increased from 0.5-0.6 to 0.8, suggesting that the specificity of adsorption inverse-phenomenon is characteristic for each food material.

Figure 3 shows Gibbs free energy changes as a function of temperature and equilibrium moisture content of roasted coffee beans and ground roasted coffee at different particle sizes.
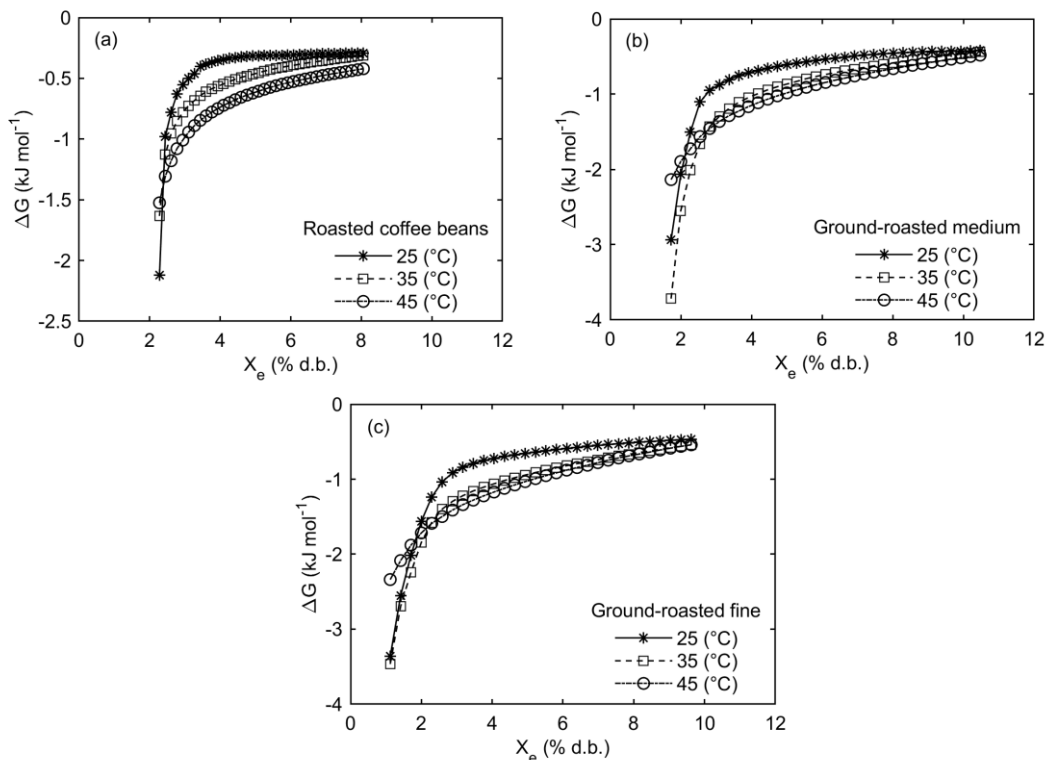
FIGURE 3. Gibbs free energy of roasted coffee beans (a), ground roasted at medium (b), and ground roasted at fine (c) particle sizes at 25, 35 and 45 °C as a function of the equilibrium moisture content

The Gibbs free energy (ΔG) represents the affinity of adsorbing materials to water molecules; the negative values are commonly associated with the spontaneous exothermic process, which does not require an input of energy from the surrounding environment (Cheng et al., 2020). As can be seen in Figure 3, the ΔG tends to zero as the equilibrium moisture content is increased for roasted coffee beans, roasted ground coffee at medium and fine particle size, indicating the lower possibility of available sorption sites at higher moisture levels (Cano-higuita et al., 2013). Moreover, the ΔG negative values indicated the spontaneous adsorption nature in roasted specialty coffee. Similar Gibbs free energy behavior has been reported in roasted coffee (de Oliveira et al., 2016), dried and roasted cocoa beans (Collazos-Escobar et al., 2020), spray-dried mango mix powders (Cano-higuita et al., 2013), and whole black peppercorns (Yogendrarajah et al., 2015).

As mentioned above for the structure effect on hygroscopic capacity, through Figure 3, this hypothesis can be confirmed. It can be observed differences in ΔG values for roasted coffee beans and ground coffee. A higher decrease of ΔG (energy released) with the increase in the moisture content of ground material respect to beans was evident. According to the criterion of spontaneity ($\Delta G < 0$), lower Gibbs free energy values indicated higher hygroscopicity. Based on this, it can be inferred that when roasted coffee

beans were ground, the specific surface area of adsorption increases, promoting the binding of more water molecules on more available number adsorption sites (Figure 2b) with higher energy as illustrated in Figure 2a.

4. CONCLUSIONS

The water vapor adsorption behavior of roasted coffee beans and ground roasted at medium and fine particle size exhibited type III shape according to Brunauer-Emmett-Teller (BET) classification, typical of rich sugar food products. An inverse temperature effect on water vapor adsorption isotherms was manifested at high water activities, which according to the literature should be ascribed to the possible sugar dissolution and the interactions of adsorbate-adsorbent in roasted specialty coffee that affected the adsorption mechanism.

The adsorption isotherms were satisfactorily modeled by Peleg equation, which provided the best goodness and can be used as a valuable tool to predict and optimize the storage conditions for water activities between 0.1 to 0.9 and temperatures of 25, 35 and 45 °C. Due to the inverse adsorption phenomenon, the theoretical GAB model was not able to describe adequately the adsorption process.

Ground coffee evidenced higher differential entropy associated with a larger number of polar available adsorption sites compared to coffee beans, and also presented higher net isosteric heat of adsorption, which is explained by a larger spontaneity (Gibbs free energy) during the hydration process.

From the thermodynamic analysis and modeling of water vapor adsorption isotherms, it was manifested the protective role of the bean-structure against the water vapor adsorption compared to the ground material. Consequently, the results of this study revealed that in order to guarantee coffee stability, the storage of the beans should be the primary option.

ACKNOWLEDGMENTS

5. REFERENCES

Aouaini, F.; Knani, S.; Yahia, M. B., Lamine, A. B. 2015. Statistical physics studies of multilayer adsorption isotherm in food materials and pore size distribution. *Physica A*, **432:** 373–390.

Arslan-Tontul, S. 2020. Moisture sorption isotherm, isosteric heat and adsorption surface area of whole chia seeds. *Lwt*, **119**: 108859.

Barbosa, M. de S. G.; Scholz, M. B.; dos S.; Kitzberger, C. S. G.; Benassi, M. de T. 2019. Correlation between the composition of green Arabica coffee beans and the sensory quality of coffee brews. *Food Chemistry*, **292:** 275–280.

Bastıoğlu, A. Z.; Koç, M.; Kaymak, F. 2017. Moisture sorption isotherm of microencapsulated extra virgin olive oil by spray drying. *Journal of Food Measurement and Characterization*, **0:**, 0.

Bon, J.; Vaquiro, H. H. A.; Mulet, A. 2012. MODELING SORPTION ISOTHERMS AND ISOSTERIC HEAT OF SORPTION OF MANGO PULP CV. *Biotecnología en el Sector Agropecuario y Agroindustrial,* **10(2):** 34–43.

Cano-higuita, D. M.; Villa-Vélez, H. A.; Telis-romero, J.; Alexander, H.; Regina, V.; Telis, N. 2013. Food and Bioproducts Processing Influence of alternative drying aids on water sorption of spray dried mango mix powders : A thermodynamic approach. *Food and Bioproducts Processing*, **93:,** 19–28.

Červenka, L.; Hloušková, L.; Žabčíková, S. 2015. Moisture adsorption isotherms and thermodynamic properties of green and roasted Yerba mate (Ilex paraguariensis). *Food Bioscience*, **12:** 122–127.

Červenka, L.; Stępień, A.; Frühbauerová, M.; Velichová, H.; Witczak, M. 2019. Thermodynamic properties and glass transition temperature of roasted and unroasted carob (Ceratonia siliqua L.) powder. *Food Chemistry*, **300:**, 125208.

Cheng, X.; Zhang, M.; Adhikari, B. 2020. Moisture adsorption in water caltrop (Trapa bispinosaRoxb.) pericarps: Thermodynamic properties and glass transition. *Journal of Food Process Engineering*, *March*, 1–11.

Clemente, G.; Bon, J.; Benedito, J.; Mulet, A. 2009. Desorption isotherms and isosteric heat of desorption of previously frozen raw pork meat. *Meat Science*, **82(4):** 413–418.

Collazos-Escobar, G. A.; Gutiérrez-Guzmán, N.; Váquiro-Herrera, H. A.; Amorocho-Cruz, C. M. 2020. Water dynamics adsorption properties of dried and roasted cocoa beans (theobroma cacao L.). *International Journal of Food Properties*, **23(1)**: 434–444.

Collazos-Escobar, G. A.; Gutiérrez-Guzman, N.; Vaquiro Herrera, H. A. 2019. MODELING DYNAMIC ADSORPTION ISOTHERMS AND THERMODYNAMIC PROPERTIES OF SPECIALTY GROUND ROASTED-COFFEE (Coffee Arabica L.). *Coffee Science*, **14(1)**: 93.

Craig, A. P.; Botelho, B. G.; Oliveira, L. S.; Franca, A. S. 2018. Mid infrared spectroscopy and chemometrics as tools for the classification of roasted coffees by cup quality. *Food Chemistry*, **245**:, 1052–1061.

Di Donfrancesco, B.; Gutierrez Guzman, N.; Chambers, E. 2014. Comparison of results from cupping and descriptive sensory analysis of colombian brewed coffee. *Journal of Sensory Studies*, **29(4):** 301–311.

Domian, E.; Brynda-kopytowska, A.; Cie, J.; Agata, G. 2018. *Effect of carbohydrate type on the DVS isotherm-induced phase transitions in spray-dried fat- fi lled pea protein-based powders.* **222.**

Sormoli, E. M.; Langrish, T. A. G. 2015. Moisture sorption isotherms and net isosteric heat of sorption for spray-dried pure orange juice powder. *LWT - Food Science and Technology*, **62(1):** 875–882.

Fan, F.; Mou, T.; Nurhadi, B.; Roos, Y. H. 2017. Water sorption-induced crystallization, structural relaxations and strength analysis of relaxation times in amorphous lactose/whey protein systems. *Journal of Food Engineering*, **196:** 150–158.

Fan, K.; Zhang, M.; Bhandari, B. 2019. Osmotic-ultrasound dehydration pretreatment improves moisture adsorption isotherms and water state of microwave-assisted vacuum fried purple-fleshed sweet potato slices. *Food and Bioproducts Processing*, **115:** 154–164.

García-Alamilla, P.; Lagunes-Gálvez, L. M.; Barajas-Fernández, J.; García-Alamilla, R. 2017. Physicochemical changes of cocoa beans during roasting process. *Journal of Food Quality*. **2969324**

Geeraert, L.; Berecha, G.; Honnay, O.; Aerts, R. 2019. Organoleptic quality of Ethiopian Arabica coffee deteriorates with increasing intensity of coffee forest management. *Journal of Environmental Management*, **231:**, 282–288.

de Oliveira, H.H. G.; Cesar, P.; de Oliveira, R. L. A. P.; Baptestini, M. F.; Vargas-Elias, A. G. 2016. ROASTING , GRINDING , AND STORAGE IMPACT ON THERMODYNAMIC

PROPERTIES AND ADSORPTION. *Journal of Food Processing and Preservation*. **00:** 1–12.

Herman, C.; Spreutels, L.; Turomzsa, N.; Konagano, E. M.; Haut, B. 2018. Convective drying of fermented Amazonian cocoa beans (Theobroma cacao var. Forasteiro). Experiments and mathematical modeling. *Food and Bioproducts Processing*, **108:** 81–94.

Iaccheri, E.; Laghi, L.; Cevoli, C.; Berardinelli, A.; Ragni, L.; Romani, S.; Rocculi, P. 2015. Different analytical approaches for the study of water features in green and roasted coffee beans. *Journal of Food Engineering*, **146:** 28–35.

Iaccheri, E.; Ragni, L.; Cevoli, C.; Romani, S.; Dalla Rosa, M.; Rocculi, P. 2019. Glass transition of green and roasted coffee investigated by calorimetric and dielectric techniques. *Food Chemistry*, **301:**, 125187.

International Coffee Organization OIC. 2020. Historical data on the global Coffee trade information. Available: http://www.ico.org/new_historical.asp?section=Statistics. Accessed 27 August 2020.

Mutlu, C.; Candal-Uslu, C.; Kılıç-Büyükkurt, Ö.; Erbaş, M. 2020. Sorption isotherms of coffee in different stages for producing Turkish coffee. *Journal of Food Processing and Preservati*on, **00:** e14440

Özdestan, Ö.; van Ruth, S. M.; Alewijn, M.; Koot, A.; Romano, A.; Cappellin, L.; Biasioli, F. 2013. Differentiation of specialty coffees by proton transfer reaction-mass spectrometry. *Food Research International*, **53(1):** 433–439.

Rodríguez-Bernal, J. M.; Flores-Andrade, E.; Lizarazo-Morales, C.; Bonilla, E.; Pascual-Pineda, L. A.; Gutierréz-López, G.; Quintanilla-Carvajal, M. X. 2015. Moisture adsorption isotherms of the borojó fruit (Borojoa patinoi. Cuatrecasas) and gum arabic powders. *Food and Bioproducts Processing*, **94:** 187–198.

Specialty Coffee Association SCA. 2020. Coffee standards. URL Available on: <https://sca.coffee/research/coffee-standards>.[Access on: 9 September 2020]

Shittu, T. A.; Idowu-adebayo, F.; Adedokun, I. I.; Alade, O. 2015. Water vapor adsorption characteristics of starch À albumen powder and rheological behavior of its paste. *Nigerian Food Journal*, 1–7.

Tao, Y.; Wu, Y.; Yang, J.; Jiang, N.; Wang, Q.; Chu, D.; Han, Y.; Zhou, J. 2018. Thermodynamic sorption properties, water plasticizing effect and particle characteristics of blueberry powders produced from juices , fruits and pomaces. *Powder Technology*, **323:** 208–218.

Tolessa, K.; Rademaker, M.; De Baets, B.; Boeckx, P. 2016. Prediction of specialty coffee cup quality based on near infrared spectra of green coffee beans. *Talanta*, **150:** 367–374.

Tripetch, P.; Borompichaichartkul, C. 2019. Effect of packaging materials and storage time on changes of colour, phenolic content, chlorogenic acid and antioxidant activity in arabica green coffee beans (Coffea arabica L. cv. Catimor). *Journal of Stored Products Research*, **84:** 101510.

Velásquez, S.; Peña, N.; Bohórquez, J. C.; Gutierrez, N.; Sacks, G. L. 2019. Volatile and sensory characterization of roast coffees – Effects of cherry maturity. *Food Chemistry*, **274**: 137–145.

Velázquez-Gutiérrez, S. K.; Figueira, A. C.; Rodríguez-Huezo, M. E.; Román-Guerrero, A.; Carrillo-Navas, H.; Pérez-Alonso, C. 2015. Sorption isotherms, thermodynamic properties and glass transition temperature of mucilage extracted from chia seeds (Salvia hispanica L.). *Carbohydrate Polymers*, **121:** 411–419.

Yao, K.; Anthony, J.; Maghirang, R.; Hagstrum, D.; Zhu, K. Y.; Bhadriraju, S. 2020. Using dynamic dewpoint isotherms to determine the optimal storage conditions of inert dust-treated hard red winter wheat. *Grain & Oil Science and Technology*.

Yogendrarajah, P.; Samapundo, S.; Devlieghere, F.; De Saeger, S.; De Meulenaer, B. 2015. Moisture sorption isotherms and thermodynamic properties of whole black peppercorns (Piper nigrum L.). LWT - Food Science and Technology, **64(1):** 177–188.